being straight lines, reflecting the nonlinear character of the system.

The rich variety of behaviour shown by this class of systems would justify a dedicated study. We are more interested in its value as a tool to study intermittent percolation processes in different physical systems where transport is not understood: for each problem, the choice of the physical meaning of U and δ, growing rate for the beasts, diffusion coefficient for U and the proper geometry will allow us to test possible mechanisms in a fully nonlinear regime. Moreover, comparison of the regime charts of very different physical systems might enlighten us as to the role played by each parameter. In our example, one clearly sees that as c, which characterizes the instability's growth rate, increases, the system's behaviour follows a route to chaos (attracting point, cycle, torus and eventually chaotic attractor); on the other hand, the entering flux ϕ_{in} (here, the total heating power provided to the plasma) forces the system from chaos into order: as the value of ϕ_{in} increases, the 'level of chaoticity' decreases.

The present behaviour can be intuitively understood from the strong correlation of the diffusion coefficient χ with the beasts' amplitude δ, and the rather weak dependence of the growth rate Γ on $(|\nabla U/G_0| - 1)$. It is likely that such charts are not always alike: other systems may have more complex regimes, for instance a trajectory in the integral map with two distinct attracting points. The integral maps themselves are powerful diagnostics of global behaviour. A measure of the percolation efficiency (or conversely of the confinement efficiency) is given by W/ϕ_{in}: in a fusion plasma, this would be analogous to the energy confinement time τ_E.

Our examples are idealized. Taking into account the real locations of resonant surfaces for realistic plasma profiles and real plasma instabilities will lead to predictions directly comparable to tokamak experiments, and we believe that the model will be useful for many other problems in physics. □

Received 23 December 1991; accepted 11 May 1992.

1. Chaté, H. & Manneville, P. *Prog. theor. Phys.* **87**, 1-60 (1992).
2. Wolfram, S. *Physica* D**10** 1-35 (1984).
3. White, R. B. *Basic Plasma Physics I* (eds Galeev, A. A. & Sudan, R. N.) 611-676 (North-Holland, Amsterdam, 1983).
4. Beaufumé, P., Dubois, M. A. & Mohamed Benkadda, M. S. *Phys. Lett.* A**147**, 87-91 (1990).
5. Rebut, P. H., Brusatti, M., Hugon, M. & Lallia, P. P. *Proc. 11th Int. Conf. Plasma Phys. Controlled Nuclear Fusion Res.*, 187 (IAEA, Vienna, 1987).
6. Fromont, B. & Beaufumé, P. *MIT Res. Rep.* 91-15; *Computers Phys.* (submitted).

Origin of ferroelectricity in perovskite oxides

Ronald E. Cohen

Geophysical Laboratory, Carnegie Institution of Washington, 5251 Broad Branch Road NW, Washington DC 20015, USA

FERROELECTRIC materials are characterized by a switchable macroscopic polarization. Most technologically important ferroelectrics are oxides with a perovskite structure. The origin of their ferroelectric behaviour is unclear, however, and there is incomplete understanding of why similar, but chemically different, perovskites should display very different ferroelectric behaviour. The great sensitivity of ferroelectrics to chemistry, defects, electrical boundary conditions and pressure arises from a delicate balance between long-range Coulomb forces (which favour the ferroelectric state) and short-range repulsions (which favour the nonpolar cubic structure). To model the transition accurately, total-energy techniques are required which incorporate the effects of charge distortion and covalency. Here I report results of electronic-structure calculations on two classic examples of ferroelectric perovskites, $BaTiO_3$ and $PbTiO_3$, and demonstrate that hybridization between the titanium 3*d* states and the oxygen 2*p* states is essential for ferroelectricity. The different ferroelectric phase behaviour of the two materials is also clear: in $PbTiO_3$, the lead and oxygen states hybridize, leading to a large strain that stabilizes the tetragonal phase, whereas in $BaTiO_3$ the interaction between barium and oxygen is completely ionic, favouring a rhombohedral structure.

Ferroelectric perovskites provide well known examples of displacive transitions[1]. The oxides $BaTiO_3$ and $PbTiO_3$ have similar cohesive properties such as unit-cell volume (64.2 and 63.2 Å^3, respectively), but different ferroelectric behaviour which has never been understood. Both are paraelectric (nonpolar) at high temperatures and have the cubic perovskite structure which is simple cubic (space group Pm3m) with 'A cations' (e.g. Pb and Ba) in the large eightfold coordinated site at (0, 0, 0), 'B cations' (e.g. Ti) in the octahedrally coordinated site at (0.5, 0.5, 0.5), and oxygens at the equipoint (0.5, 0.5, 0). $BaTiO_3$ has three ferroelectric phase transitions, cubic to tetragonal (393 K), tetragonal to orthorhombic (278 K) and orthorhombic to rhombohedral (183 K), whereas $PbTiO_3$ has only one, cubic to tetragonal at 766 K. The ferroelectric distortions involve small displacements of the cations relative to the anions, leading to a net dipole moment per unit volume, or polarization. The displacements are similar in the tetragonal phases for the two materials, although larger in $PbTiO_3$ (refs 2, 3).

Both materials are also ferroelastic: tetragonal $BaTiO_3$ has a 1% c/a strain, whereas tetragonal $PbTiO_3$ shows a large (6%) strain. Typical ferroelastics show strains of 0.5-3% (ref. 4). The relative contributions of the elastic energy, long-range coulomb interactions and local bonding effects to the phase transitions are not known. Also unclear is whether the dynamics should be described as order-disorder or displacive near the phase transitions. The ferroelectric phase transitions in perovskites were long considered prototypical displacive transitions, characterized by a zone-centre vibrational mode, the 'soft mode', with a vanishing frequency at the phase transition and an eigenvector similar to the displacements observed in the ferroelectric phases. Recent work, however, focuses on the order-disorder 'eight-site' model[5], in which the cubic phase consists of random distortions along eight cube diagonals [111], the tetragonal phase consists of displacements along four cube diagonals giving an average structure with a polarization along [100], the orthorhombic phase has two 'sites' occupied and a polarization along [110], and the rhombohedral phase is ordered along [111].

To ascertain whether this model was appropriate for both $BaTiO_3$ and $PbTiO_3$, I used the all-electron, full-potential, linearized augmented plane-wave method[6] within the local density approximation (LDA) for the exchange and correlation interactions between electrons[7]. The computations make no assumptions about bonding, ionicity, or the shape of the charge density or potential, and are essentially fully converged. For previous calculations on $BaTiO_3$ that include extensive convergence tests, see ref. 8.

Ideally the entire parameter space for zone centre and zone boundary distortions, including interactions with volume and shear strains, would be mapped from first principles to predict the phase transition temperatures and average dynamical behaviour; this is not technically feasible, so I have used the experimental distortions as a guide, and consider here only rhombohedral and tetragonal zone-centre distortions.

Figure 1 shows the energy against the experimental distortion for $BaTiO_3$ and $PbTiO_3$, with and without tetragonal c/a strain. Without the strain, both $BaTiO_3$ and $PbTiO_3$ give the lowest energy for the rhombohedral structure. Energetically the rhombohedral strain is small (it contributes less than 11 K to the energy differences), but the tetragonal strain has a considerable effect in $BaTiO_3$, and in $PbTiO_3$ it stabilizes the tetragonal structure over the rhombohedral phase. In the high-temperature phases, the underlying multiple-well structure of the potential surface still exists. These phases in both $BaTiO_3$ and $PbTiO_3$

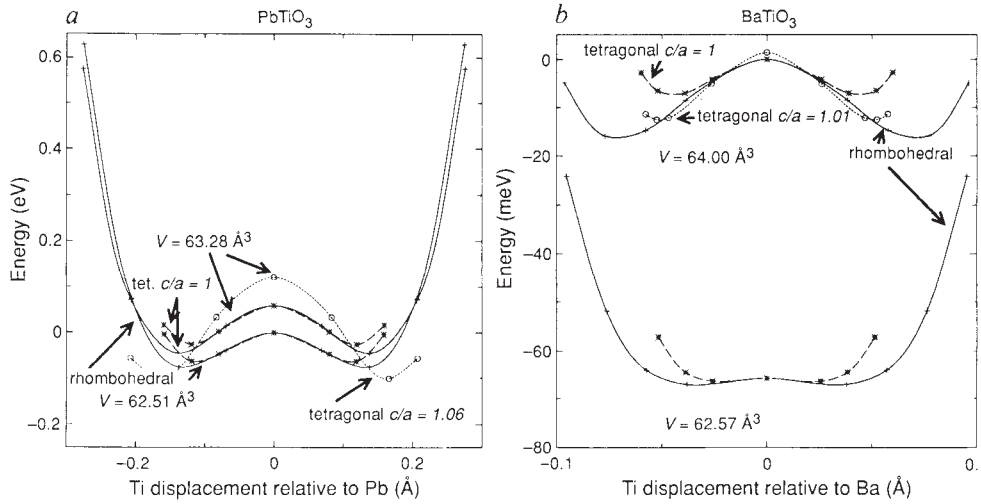

FIG. 1 Calculated energy as a function of soft-mode distortion in (*a*) $PbTiO_3$ and (*b*) $BaTiO_3$. The $PbTiO_3$ wells are much deeper than for $BaTiO_3$. In both $BaTiO_3$ and $PbTiO_3$ without strain the rhombohedral phase has lower energy. In $PbTiO_3$, however, tetragonal strain stabilizes the tetragonal phase over the rhombohedral phase. In $BaTiO_3$ strain has a much smaller effect and the rhombohedral phase is still lower in energy. The large volume effect (pressure decreases the well depths) is more obvious in $BaTiO_3$ because of the smaller energy scale.

are anharmonic, disordered crystals with the atoms seldom in their idealized cubic positions; the ions are mostly displaced along the [111] directions. The tetragonal phase in $PbTiO_3$ is ordered because of the large stabilizing strain (the strained experimental structure is more than 1,800 K lower in energy than the cubic structure), but in $BaTiO_3$ the corresponding energy difference is only ~150 K, and only the low-temperature rhombohedral phase is expected to be well ordered, as seen by experiment[5].

Figure 1 also shows the large volume dependence of the soft-mode potential surfaces, consistent with the loss of ferroelectricity in the titanates at high pressures[9]. The ferroelectric to paraelectric transition with pressure is different from the thermally induced transition. Under compression the multiple-well structure disappears, and a continuous transition at zero temperature occurs at the pressure where the well depths vanish; as the low-pressure transition is first-order, there is a tricritical point where the transition changes from first-order to continuous[10]. The large sensitivity to volume makes the volume errors in LDA (here 2-4%) unusually important, and the calculated ground state may in some cases be only slightly distorted or even cubic. Other studies indicate that good estimates of vibrational frequencies and elastic constants are obtained using the LDA for the experimental lattice[11,12]. Better approximations for exchange correlation would reduce the uncertainty.

I found the elements of the dynamical matrix, expanded around the experimental tetragonal structure of $PbTiO_3$, by 'frozen phonon' displacements of the atoms, and the matrix was diagonalized giving the eigenmode frequencies within the harmonic approximation. The three computed A_1 frequencies (displacements in the polar direction) at 142, 446 and 663 cm^{-1} and the four E frequencies (transverse displacements) at 75, 190, 250 and 480 cm^{-1}, are similar to the experimental values[13] of 148, 362, 650, 89, 220, 290 and 508 cm^{-1}, respectively. The discrepancies are probably due to the anharmonic shape of the potential surface. The lowest frequency is stable, indicating the absence of lower-temperature transitions. $BaTiO_3$, which does have lower-temperature transitions, is still dynamically unstable in the tetragonal phase as the ferroelectric distortions are small.

The electronic densities of states (Fig. 2) indicate that Ti 3*d* states are strongly hybridized with the O 2*p* and that the hybridization is enhanced by the ferroelectric distortion. The sum of the band eigenvalues is one term in the total energy (the sum double-counts the coulomb potential and includes the exchange-correlation potential functional rather than the energy functional)[14], and it clearly decreases with the ferroelectric distortion due to the Ti-O bonding interaction. It is striking to compare the partial densities of states of $PbTiO_3$ with $BaTiO_3$ using the experimental $PbTiO_3$ structure for both, so that differences are due entirely to the replacement of Ba and Pb. Lead 6*s* and O

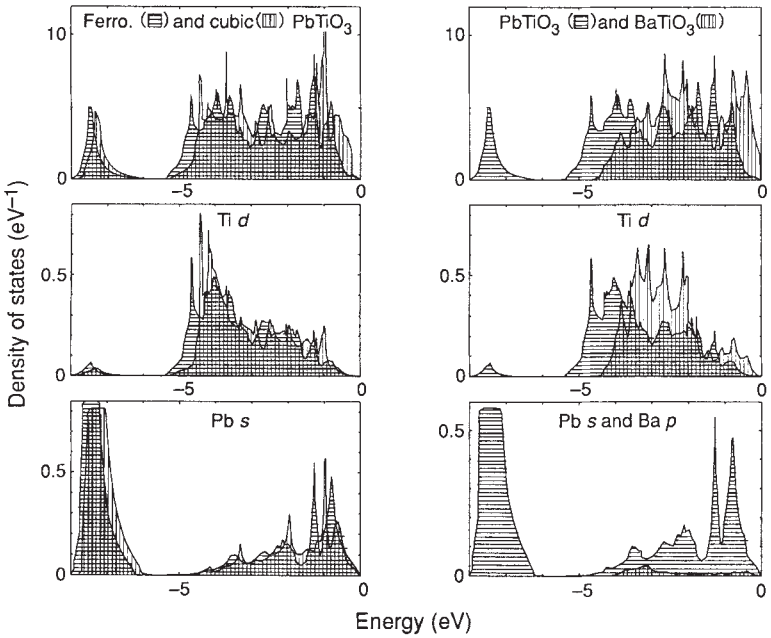

FIG. 2 Electronic density of states against energy relative to the valence-band maxima for (*a*) ferroelectric $PbTiO_3$ (horizontal stripes) and cubic $PbTiO_3$ (vertical stripes), and (*b*) ferroelectric $PbTiO_3$ (horizontal) and $BaTiO_3$ (vertical stripes). The top panels show the total densities of states and the bottom two show the contributions (partial densities of states) from the regions around the Ti for states with *d* character and around Pb or Ba with *s* or *p* character, respectively. Overlap of the Ti 3*d* and Pb 6*s* partial densities of states with the primarily oxygen 2*p* valence bands, which range from 0 to ~ −5.5 eV, indicates considerable hybridization. The ferroelectric distortion also lowers the eigenvalue sum, helping to decrease the total energy. The $PbTiO_3$ structure was used for $BaTiO_3$ to obtain the results in the right panels (*b*) so that the differences are due solely to the replacement of Pb by Ba; whereas the Pb *s* state is strongly hybridized with the oxygen 2*p* states, the Ba is fully ionic. The Ti-O interactions are also different in $BaTiO_3$ and $PbTiO_3$ even with the same structure, because they are influenced in the latter by the Pb-O interaction.

$2p$ states are strongly hybridized in $PbTiO_3$, but Ba $5p$ does not hybridize with the valence band. The Pb–O bonding interaction, and the smaller ionic radius of Pb^{2+} compared with Ba^{2+}, lead to the larger strain in $PbTiO_3$ that reduces some Pb–O distances; the Ti–O repulsion prevents the volume shrinking enough to stabilize the cubic phase. There is also an indirect effect on the Ti–O interactions through the Pb–O hybridization; the Ti $3d$ eigenvalues are lower in $PbTiO_3$ relative to $BaTiO_3$ even for the same atomic displacements.

My calculations do not support the idea that the ferroelectric distortion is due to the B cation 'rattling' in the oxygen cage[15] and that the volume is constrained by the A-cation repulsions with oxygen, nor is this idea consistent with radius ratio arguments. The shortest Ti–O distances in the experimental tetragonal structures of $BaTiO_3$ and $PbTiO_3$ are 1.86 and 1.78 Å, respectively, significantly smaller than the 2.00 Å expected from the Shannon and Prewitt (S–P) ionic radii[16], whereas the shortest Ba–O and Pb–O distances are 2.79 and 2.53 Å, comparable to the S–P radii (2.82 and 2.69 Å).

The valence charge on the Ti, its polarization, and the dynamical nature of the covalency and polarization, are evident in the charge density (Fig. 3). Dipolar electron density around the Pb (hybrid Pb–O states) develops with increasing ferroelectric distortion. In contrast, Ba does not polarize with the ferroelectric distortion. In both materials the Ti strongly distorts and bonds with the closer oxygen. Ti is not fully ionized as a 4+ ion; fits to the self-consistent charge density give $O^{-1.63}$ and $Ti^{+2.89}$.

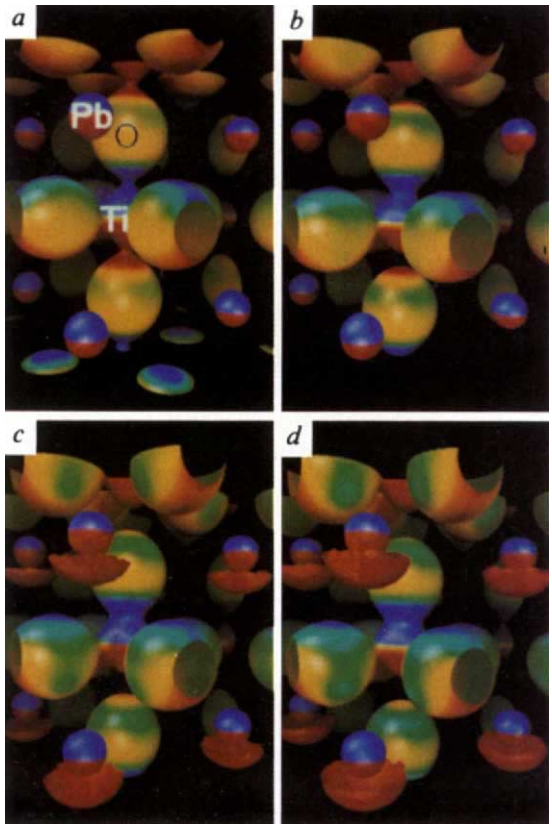

FIG. 3 Valence charge density of $PbTiO_3$ for increasing ferroelectric distortions (all with $c/a=1.06$). The O and Ti atoms are displaced towards the bottom of the figure. Panels a–d correspond to the four strained tetragonal points in Fig. 1a. Constant density surfaces for 0.26 electrons $Å^{-3}$ are shown. The charge density corresponds to the oxygen $2p$ bands as well as the Pb s band. The most important features are the significant valence charge density on the Ti (Ti^{4+} would have essentially no valence charge) and the clear polarization of the Pb ions. A similar distortion does not occur around the Ba in $BaTiO_3$. The colours give the z-component of the electric field at each point on the surface. Near the nuclei the electric field is dominated by the nuclear field, but at greater distances the asymmetry between the red and blue colouring indicates the periodic field that forms in the crystal because of the ferroelectric distortion. A finite crystal could also develop a macroscopic field, depending on the surface boundary conditions.

If the Ti–O hybridization is inhibited, the ferroelectric instability disappears and the cubic phase is most stable. This has been shown in two ways. Non-empirical model calculations using the 'potential induced breathing' model, which assume spherical ions and no covalency, give no ferroelectric state for either $BaTiO_3$ (ref. 17) or $PbTiO_3$. Analysis of the results shows that although the long-range Coulomb (Madelung) energy favours a ferroelectric distortion, the short-range repulsions are strong enough to stabilize the cubic phase. Second, in calculations using the linearized augmented plane-wave method if the Ti d energy parameter is raised to reduce the variational freedom, the ferroelectric state is lost, indicating the importance of the Ti d-states for the instability. We can conclude that for ferroelectric perovskites in general, hybridization between the B cation and O is essential to weaken the short-range repulsions and allow the ferroelectric transition. Most ferroelectric oxide perovskites have B cations whose lowest unoccupied states are d-states (Ti^{4+}, Nb^{5+}, Zr^{4+} and so on). This allows for d-hybridization with the O that softens the B–O repulsion and allows the ferroelectric instability at low pressures. The A-cation can modify the ground state and nature of the transition by (1) increasing the ferroelastic strain that couples with the ferroelectric distortions or (2) hybridizing with the valence states, leading indirectly to changes in the B–O interactions. The delicate balance of short-range forces favouring the cubic phase and long-range forces favouring the ferroelectric state makes the transition sensitive to defects that modify the short-range interactions and to carriers (e.g. photoelectrons) that screen the long-range field.

As the temperature of rhombohedral ground-state perovskites such as $BaTiO_3$ and $KNbO_3$ is raised, the atoms tend to average over the low-energy [111] distortions, leading to a series of phase transitions. Even in cases with small strain, such as $BaTiO_3$, the strain energy strongly affects the phase transitions[18]. In tetragonal ground-state pervoskites such as $PbTiO_3$, the strain is larger and stabilizes an ordered tetragonal phase; at high temperatures, however, the cubic phase $PbTiO_3$ also has an underlying multiple-well potential surface and should be anharmonic, as is observed. The strain changes the equilibrium phase diagram and should also damp the local fluctuations in the ferroelectric phases. Underlying anharmonic potential surfaces, leading to high-temperature phases with atoms that seldom sit on their equilibrium positions, are not unique to ferroelectrics, and also typify rotational instabilities in perovskites and the tilt instabilities in the cuprate superconductors[19]. □

Received 11 March; accepted 8 May 1992.

1. Lines, M. E. & Glass, A. M. *Principles and Applications of Ferroelectrics and Related Materials* (Clarendon, Oxford, 1977).
2. Shirane, G., Pepinsky, R. & Frazer, B. C. *Acta crystallogr.* **9,** 131–140 (1956).
3. Harada, J., Pedersen, T. & Barnea, Z. *Acta crystallogr.* A**26,** 608–612 (1970).
4. Salje, E. K. H. *Phase Transitions in Ferroelastic and Co-elastic Crystals* (Cambridge Univ. Press, 1990).
5. Comes, R., Lambert, M. & Guinier, A. *Acta crystallogr.* A**26,** 244–254 (1970).
6. Wei, S.-H. & Krakauer, H. *Phys. Rev. Lett.* **55,** 1200–1203 (1985).
7. Hedin, L. & Lundqvist, B. I. *J. Phys.* C**4,** 2064–2083 (1971).
8. Cohen, R. E. & Krakauer, H. *Phys. Rev.* B**42,** 6416–6423 (1990).
9. Decker, D. L. & Zhao, Y. X. *Phys. Rev.* B**39,** 2432–2438 (1989).
10. Ramirez, R., Lapeña, M. F. & Gonzalo, J. A. *Phys. Rev.* B**42,** 2604–2606 (1990).
11. Cohen, R. E., Pickett, W. E. & Krakauer, H. *Phys. Rev. Lett.* **64,** 2575–2578 (1990).
12. Cohen, R. E. in *High Pressure Research: Application to Earth and Planetary Science* (eds Syono, Y. & Manghnani, M. H.) (Terra Scientific, Tokyo, 1992).
13. Fontana, M. D., Idrissi, H., Kugel, G. E. & Wojcik, K. *J. Phys.: Condens. Matter* **3,** 8695–8705 (1991).
14. Kohn, W. & Vashishta, P. in *Theory of the Inhomogeneous Electron Gas* (eds Lundqvist, S. & March, N. H.) (Plenum, New York, 1983).
15. Slater, J. C. *Phys. Rev.* **78,** 748–761 (1950).
16. Shannon, R. D. & Prewitt, C. T. *Acta crystallogr.* B**25,** 925–946 (1969).
17. Boyer, L. L., Mehl, M. J., Flocken, J. W. & Hardy, J. R. *J. appl. Phys.* **24,** Suppl. 24-2, 204–205 (1985).
18. Marais, S., Heine, V., Nex, C. & Salje, E. *Phys. Rev. Lett.* **66,** 2480–2483 (1991).
19. Pickett, W. E., Cohen, R. E. & Krakauer, H. *Phys. Rev. Lett.* **67,** 228–231) (1991).

ACKNOWLEDGEMENTS. I thank L. L. Boyer, R. J. Hemley, H. Krakauer, W. E. Pickett, and D. Singh for discussions and H. Krakauer, R. M. Hazen and C. T. Prewitt for reading the manuscript. Computations were done on the Cray 2 at the National Center for Supercomputing Applications under the auspices of the NSF. This research was supported by the Office of Naval Research.